Augmented L1 adaptive control of an actuated knee joint exoskeleton: From design to real-time experiments

Hala Rifaï, Mohamed Sabri Ben Abdessalem, Ahmed Chemori, Samer Mohammed, Yacine Amirat

Augmented $\mathcal{L}1$ Adaptive Control of an Actuated Knee Joint Exoskeleton: From Design to Real-Time Experiments

H. Rifaï[1], M.S. Ben Abdessalem[1], A. Chemori[2], S. Mohammed[1] and Y. Amirat[1]

***Abstract*— This paper deals with the control of a lower limb exoskeleton acting on the knee joint level. Classical $\mathcal{L}1$ adaptive control law is proposed to ensure assistance-as-needed and resistive rehabilitation following a desired trajectory considered defined by a therapeutic doctor. This control law introduces a time lag within the desired trajectory tracking because of the presence of a filter in its structure. In order to mitigate this drawback, the classical $\mathcal{L}1$ adaptive control is augmented by a nonlinear proportional control. The classical and augmented $\mathcal{L}1$ adaptive control laws are tested in real-time using the exoskeleton EICOSI of LISSI-lab. Real-time experimental results highlight the utility of these control laws in assistance-as-needed and resistive rehabilitation. They also show the effectiveness of the augmented version of the $\mathcal{L}1$ adaptive control.**

I. INTRODUCTION

The ageing of the societies and the high percent of disabilities have encouraged the development of exoskeletons [1]. These external skeletal systems can be used in rehabilitation but also in performance enhancement. Within the first application, they enable the wearer to regain control of his/her limbs and to perform movements that have been lost [2]. Within the second application, the exoskeletons empower the wearer and allow him to perform tasks of high endurance such as load carrying [3].

Lower limb exoskeletons act particularly on the hip, knee and ankle joints or separately on these articulations. They aim to assist the movement of the lower limbs at the impairment level during daily living activities. When the wearer develops a part of the effort necessary to perform a movement and the exoskeleton delivers the complement, the paradigm is called assistance-as-needed. The lower limb exoskeletons aim also to perform rehabilitation programs trying to restore the movement of the impaired joints. Within this context, two programs can be envisaged: passive and resistive rehabilitations. Passive rehabilitation concerns people who have completely lost control of their limbs after spinal cord injuries for example [4], [5]. The resistive rehabilitation, on the other hand, involves the wearer in the process by inviting him to develop an effort in the opposite direction of the exoskeleton's movement [6]. In both cases, the rehabilitation process is monitored by a therapist whose workload is drastically alleviated thanks to the automated process.

Different control techniques have been established to automatically drive the lower limb exoskeletons. One can cite the classical PID (proportional, integral, derivative) structure for gait assistance and its derivatives such as the proportional controller which acts as an amplifier of the human developed torque estimated using EMG (electromyogram) electrodes measurements [7], [8] and the proportional derivative controller where the wearer force is measured through shoes insoles [9]. In [2], a position and torque controllers that generate a torque proportional to the deviation angle from the desired trajectory are proposed for gait rehabilitation of hemiparetic patients, the control torque is applied only when the wearer needs to be assisted. A bounded control law that has the advantage of avoiding the saturation of the exoskeleton's actuator has been proposed in [10] to ensure passive rehabilitation of a completely disabled wearer, it allows to guarantee the security of the wearer by maintaining the functioning of the actuator in a linear mode. A quasi-passive structure of exoskeleton is presented in [11] where the stiffness of the knee is on-off controlled with respect to stance phases detected with shoe insoles. Impedance control has been also developed for exoskeletons such that the impedance of the exoskeleton-wearer system can be adapted acting on the inertia, damping or stiffness parameters [12], [13], [14]. Adaptive control has been proposed in [15] allowing to adapt all the system's (exoskeleton and wearer) parameters function of the task to perform. Adaptive strategies allow to ensure position control with a compliant wearer-exoskeleton system: the parameters are adapted continuously so that the best performance in desired trajectory tracking is ensured. Note that compliant structures of exoskeletons have been developed such that the exoskeleton's impedance can vary from very stiff to very compliant depending on the task to perform [16].

Thanks to the aforementioned advantages of the adaptive control, a $\mathcal{L}1$ adaptive position controller will be proposed in this work. Besides the parameters adaptability, the $\mathcal{L}1$ adaptive control ensures that the signals in the feedback loop remain bounded due to the projection function existing in its expression [17]. Moreover, it guarantees a transient performance and robustness in presence of parameters' fast adaptation. Robustness and adaptation are decoupled and a compromise can be set by means of a filter present in the control law structure. This filter, however, is behind the main drawback of the $\mathcal{L}1$ adaptive control because it creates a time lag within the tracking of the desired trajectory.

[1]H. Rifaï, M.S. Ben Abdessalem, S. Mohammed and Y. Amirat are with the LISSI-lab, Université de Paris-Est Créteil (UPEC), 122 rue Paul Armangot, 94400 Vitry-Sur-Seine, France, {hala.rifai, samer.mohammed, amirat}@u-pec.fr, mohamed.sabri.b.ab@gmail.com

[2]A. Chemori is with the LIRMM, Université Montpellier Sud de France (UMSF)-CNRS, 161 rue Ada, 34392 Montpellier, France, ahmed.chemori@lirmm.fr

This drawback can be mitigated by augmenting the $\mathcal{L}1$ adaptive control with a nonlinear proportional or a PI, PID controllers as proposed in [18], [19]. Among applications of the $\mathcal{L}1$ adaptive control, one can cite the aerial vehicles, the underwater vehicles, the robot manipulators, etc. [19], [20], [21].

To the authors best knowledge, the $\mathcal{L}1$ adaptive control has not been applied to wearable robots previously. In this paper, the $\mathcal{L}1$ adaptive control is applied to the Exoskeleton Intelligently COmmunicating and Sensitive to Intention (EICOSI) that has a rotational degree of freedom at the knee joint level [10].

The remainder of the paper is structured as follows. In section II, the shank-foot-exoskeleton model is recalled. The classical and augmented $\mathcal{L}1$ adaptive control laws are presented in section III. Real-time experiments using EICOSI are addressed in section IV for assistance-as-needed and resistive rehabilitation. Finally, conclusions and future works are sketched in section V.

II. SHANK-FOOT-EXOSKELETON: DESCRIPTION AND MODELING

EICOSI (cf. Fig. 1) is a lower limb exoskeleton that has a rotational degree of freedom at the knee joint level. It is driven by a brushless DC motor and is equipped with an incremental encoder to measure the knee joint angle. It is embodied by the lower limb and attached to by means of straps such that it rotates synchronously with the knee joint. The shank-foot-exoskeleton is therefore considered as an entity that is put in movement thanks to the exoskeleton actuator's torque and to the wearer's active muscular torque if present. These two torques are the shank-foot-exoskeleton system's external inputs. The wearer is considered in a seated position, the shank is hanging (cf. Fig. 4). Flexion and extension movements of the knee joint are studied in this work such that the system tracks a desired trajectory considered defined by a therapeutic doctor. Deriving the Lagrangian of the shank-foot-exoskeleton system, the rotational dynamics can be obtained [10]:

$$J\ddot{\theta} = -\tau_g \cos\theta - K(\theta - \theta_r) - A\text{sign}\dot{\theta} - B\dot{\theta} + \tau + \tau_h, \quad (1)$$

where θ is the knee joint rotation angle which is defined as the angle between the actual position of the shank and the full extension position, $\dot{\theta}$ and $\ddot{\theta}$ are the knee joint angular velocity and acceleration respectively, θ_r is the angle of the knee joint at the rest position of the shank, J is the shank-foot-exoskeleton system's moment of inertia, τ_g is the system's gravitational torque in the full extension position of the shank, K is the system's stiffness coefficient, A is the system's solid friction coefficient, B is the system's viscous friction coefficient and sign$(\cdot)$ is a signum function. τ is the control torque delivered by the exoskeleton's actuator and τ_h is the human active torque generated by his active muscles.

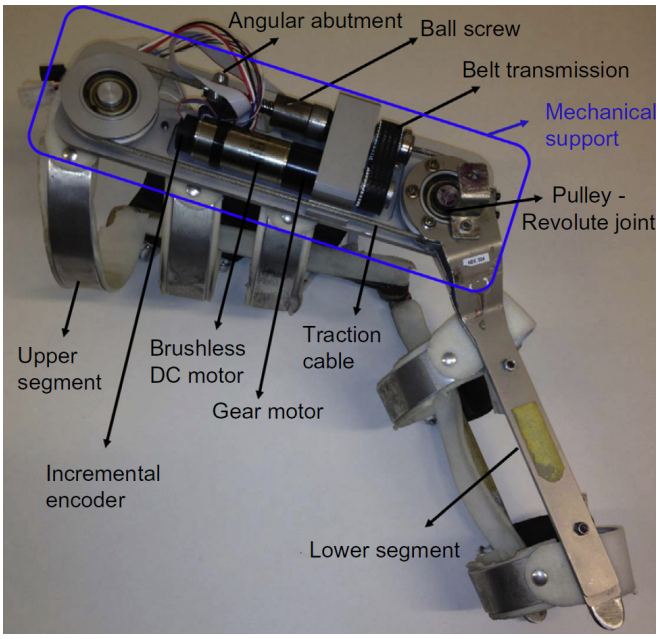

Fig. 1. View of the exoskeleton system and its components.

III. PROPOSED CONTROL SOLUTION: AUGMENTED $\mathcal{L}_1$ ADAPTIVE CONTROL

A. Background on $\mathcal{L}_1$ adaptive control

In order to avoid degradation in the closed-loop performance of a controlled system, adaptive control has been developed. Indeed, the controller is expected to possess a self tuning ability and compensate for different kind of uncertainties/disturbances and changes in the system/environment. That is why adaptive controllers are very popular for such systems. However, it is worth to emphasize various issues related to the implementation of a classical adaptive controller, such as i) the need for the persistency in excitation that can lead to a bad transient behavior, ii) the tuning of the adaptation gains that can lead either to instability (high gains) or slow down the convergence rate (small gains), iii) the need of an appropriate initialization of the estimated parameters requiring an a priori knowledge of the system. The $\mathcal{L}_1$ adaptive control [17] scheme stands out among all other developed methods in its particular architecture where robustness and adaptation are decoupled. Its architecture is constructed (inspired by Model Reference Adaptive Control) using four main parts as illustrated in Fig. 2, namely *the controlled system*, *the state predictor*, *the adaptation mechanism* and *the control law* including a low pass filter.

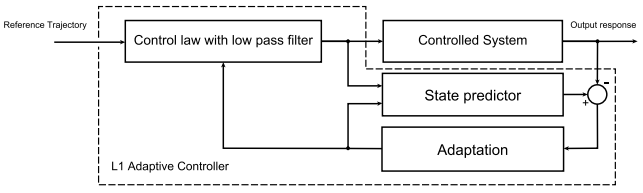

Fig. 2. View of the block diagram of $\mathcal{L}_1$ adaptive control scheme

The controlled system: Let's consider the class of systems modelled by the following dynamics :

$$\dot{x}(t) = Ax(t) + b\Big(\omega(t)u(t) + W^T(t)x(t) + \sigma(t)\Big), x(0) = x_0$$
$$y(t) = cx(t) \tag{2}$$

$x \in \mathbb{R}^n$ is the state vector which is supposed to be measurable, $u(t) \in \mathbb{R}$ is the control input, $b \in \mathbb{R}^n$ and $c \in \mathbb{R}^{1\times n}$ are constant vectors supposed to be unknown, $A \in \mathbb{R}^{n\times n}$ is a known matrix such that (A, b) is controllable, $W \in \mathbb{R}^n$ is the vector of unknown constant parameters with a known bound. $\sigma(t) \in \mathbb{R}$ is a time varying disturbance, while $\omega(t) \in \mathbb{R}$ is unknown constant with known sign, y is the system's output. Having defined a piecewise-continuous bounded reference trajectory $r(t)$, the control objective lies in the design of an adaptive state feedback input $u(t)$ so that the output $y(t)$ tracks $r(t)$ while preserving the boundedness of the states and the parameters of the system. This control input is composed of two parts defined according to the following:

$$u(t) = u_m(t) + u_a(t) \quad , \quad u_m(t) = -k_m x(t) \tag{3}$$

u_m is the component rendering the matrix A Hurwitz thanks to $k_m \in \mathbb{R}^{1\times n}$ being the static feedback gain that transforms A into $A_m = A - bk_m$. The matrix A_m is therefore the one delimiting the closed-loop dynamics of the system. It remains u_a being the adaptive control input to be designed. By combining (2) and (3), one gets:

$$\dot{x}(t) = A_m x(t) + b\Big(\omega(t)u_a(t) + W^T(t)x(t) + \sigma(t)\Big), x(0) = x_0$$
$$y(t) = cx(t) \tag{4}$$

The matrix A is replaced by the Hurwitz one A_m thanks to the incorporation of $u_m(t)$. The control input is therefore reduced to the adaptive component $u_a(t)$.

The state predictor: The states of the system are computed at every iteration based on the estimated parameters obtained from the adaptation mechanism along with the control input. The predictor is therefore constructed according to the following:

$$\dot{\hat{x}}(t) = A_m\hat{x}(t) + b\Big(\hat{\omega}(t)u_a(t) + \hat{W}^T(t)x(t) + \hat{\sigma}(t)\Big), x(0) = x_0$$
$$\hat{y}(t) = c\hat{x}(t) \tag{5}$$

$\hat{x}(t) \in \mathbb{R}^n$ is the state of the predictor of the system and $\hat{W}^T(t) \in \mathbb{R}^n$ is the estimate of the vector of unknown constant parameters. Finally $\hat{y} \in \mathbb{R}$ is the estimate of the output.

The adaptation mechanism: It uses the error between the measured and the estimated states to adapt the parameters together with a projection method in order to ensure their boundedness. Indeed, a projection operator avoids the parameter drift using the gradient of a convex function and a maximal bound on the parameters to be estimated. The adaptation law for each estimated parameter is then given by:

$$\begin{aligned}\dot{\hat{W}}(t) &= \Gamma_W Proj(\hat{W}(t), -\tilde{x}^T(t)Pbx(t))\\ \dot{\hat{\sigma}}(t) &= \Gamma_\sigma Proj(\hat{\sigma}(t), -\tilde{x}^T(t)Pb)\\ \dot{\hat{\omega}}(t) &= \Gamma_\omega Proj(\hat{\omega}(t), -\tilde{x}^T(t)Pbu_a(t))\end{aligned} \tag{6}$$

where P is the solution of the algebraic Lyapunov equation $A_m^T P + PA_m^T = -Q$ for any arbitrary symmetric matrix $Q = Q^T > 0$. $\Gamma_W, \Gamma_\sigma, \Gamma_\omega$ are the adaptation gains and $\tilde{x}(t)$ is the prediction error.

The Control law with low pass filter: This part pertains to the adaptive component of the control input characterized by the consideration of a low pass filter. It is written in Laplace form as:

$$u_a(s) = -C(s)(\hat{\eta}_l(s) - k_g r(s)) \tag{7}$$

where $C(s)$ is a bounded input, bounded output stable and strictly proper transfer function, $\hat{\eta}_l(t) = \hat{W}^T(t)x(t)$, $k_g = -\frac{1}{cA_m^{-1}b}$ and $r(s)$ the Laplace transform of the reference trajectory $r(t)$. The system (2) under the $\mathcal{L}_1$ adaptive controller proposed by (7) is guaranteed to be bounded input bounded state stable with respect to reference trajectory and initial conditions if k_m and $C(s)$ verify with following $\mathcal{L}_1$ norm condition:

$$||G(s)||_{\mathcal{L}_1} L < 1 \tag{8}$$

where

$$G(s) = H(s)(1 - C(s)), H(s) = (s\mathbb{I} - A_m)^{-1}b, L = max||\theta|| \tag{9}$$

$G(s)$ and $H(s)$ and $C(s)$ being bounded-input bounded-output stable transfer functions. L is the maximal bound set on the parameter W.

Applied to the exoskeleton EICOSI, one can write in case of a passive wearer, then developing a null active muscular torque ($\tau_h = 0$): $x = [x_1\ x_2]^T = [\theta\ \dot{\theta}]^T$, $b = [0\ 1]^T$, $A_m = \begin{bmatrix} 0 & 1 \\ -k_{m_1} & -k_{m_2}\end{bmatrix}$, $W = [-\frac{K}{J} + k_{m_1}\ -\frac{B}{J} + k_{m_2}]^T$, $\omega = \frac{1}{J}$, $\sigma = \frac{K}{J}\theta_r - \frac{\tau_g}{J}\cos x_1 - \frac{A}{J}\text{sign}x_2$ and $c = [1\ 0]$.
In case of an active wearer ($\tau_h \neq 0$), τ_h can be considered as an external disturbance and takes part of the disturbance term σ without changing the proof as it is stated in [22]. The only condition is that τ_h should be a continuously differentiable bounded with uniformy bounded derivative which is validated since τ_h is a continuous muscular bounded torque: $\tau_h \leq \Delta_h$ where Δ_h is the bound.

B. Augmented $\mathcal{L}_1$ adaptive control

To deal with the issue of time lag, which appears when the controller is applied to track a time-varying reference trajectory, as in [18], an augmentation of the $\mathcal{L}_1$ adaptive control is proposed. The augmented controller is illustrated in Fig. 3. The extension is displayed in dotted lines. A linear PI controller or a nonlinear proportional controller can be used as the additional term to be summed to the original filtered control input. The idea of the nonlinear proportional control term lies in choosing a nonlinear varying feedback gain. To get a fast transient with a small overshoot, the added control input $u_p(t)$ can chosen be, according to [23], as follows:

$$u_p(t) = -g(e, \alpha, \delta) \tag{10}$$

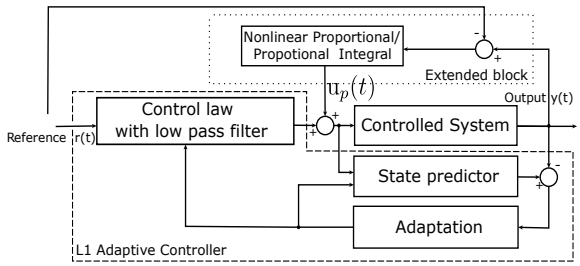

Fig. 3. Block diagram of the extended $\mathcal{L}_1$ adaptive control scheme

with

$$g(e,\alpha,\delta) = \begin{cases} a_1|e|^{\alpha}sgn(e) & \text{if } |e| > \delta \\ a_2\frac{e}{\delta^{1-\alpha}} & \text{if } |e| \leq \delta \end{cases}$$

the parameters a_1, a_2 are constant gains (they can be chosen as $a_1 = a_2$ for avoiding a discontinuity), e is the tracking error, α is a design parameter such that $0 < \alpha \leq 1$ and δ is a threshold of the transition between low and and high gains.

IV. REAL-TIME EXPERIMENTAL RESULTS

A. Experimental platform and Hardware aspects

The experiments are performed using the Exoskeleton Intelligently COmmunicating and Sensitive to Intention (EICOSI) (cf. Fig. 1). It is a lower limb exoskeleton, actuated at the knee joint level by means of a brushless DC motor. It is fixed to the wearer's leg by means of straps that attach it to the thigh and shank. EICOSI and the wearer (cf. Fig. 4) forms then an entity that moves synchronously due to two major active torques: the control torque delivered by the EICOSI's actuator and the wearer's torque developed by active thigh muscles. The quadriceps represents the extensor muscles and the hamstrings represents the flexor ones. EMG electrodes are therefore fixed at the level of the rectus femoris (RF) acting as a quandriceps muscle and the biceps femoris long head (BF) acting as hamstring muscle to show when the muscles are active during the experiments. Note that the EMG measurements are presented only to show the muscles activity and are not used in the control law computation. EICOSI is equipped with an incremental encoder that measures the rotational angle of the knee joint. The angular velocity is derived numerically. A dSPACE controller board is used to compute the pulse width modulation level to control the actuator's velocity taking as inputs the current and desired knee joint angles as well as the angular velocities. Experiments have been performed on a male subject being 23 years old, weighing 65 Kg and measuring 178 cm (cf. Fig. 4). The subject presents no spasticity or contracture of the knee joint and is therefore able to perform complete flexion and extension. He has been informed of the experiment's protocol and benefit of the study. Precautions have been taken such that the experiments preserve the subject's health. Privacy and confidentiality have been respected.

All the estimated parameters of the control torque have been initialized to zero. The parameters of the state feedback are taken as: $k_{m_1} = 1$ and $k_{m_2} = 1.4$.

Fig. 4. The shank-foot-exoskeleton system during experiments.

The classical and the augmented $\mathcal{L}1$ adaptive control laws are tested and compared in the sequel. Three case studies are presented corresponding to: i) a passive wearer who is not delivering any active muscular effort, followed by ii) an active wearer who is assisted-as-needed by the exoskeleton to perform a task or followed by iii) an active wearer who is resisting the movement of the exoskeleton in a kind of a resistive rehabilitation process.

B. Assistance-as-needed

The first two experiments are divided into two phases: in the first one, the wearer is not delivering any active muscular effort and in the second phase the wearer delivers a muscular torque that takes the shank-foot-exoskeleton system in the same direction as the desired trajectory of the exoskeleton. However, this torque is not sufficient to ensure the whole system's movement. The wearer is therefore assisted by the exoskeleton to track the desired trajectory.

First, the classical $\mathcal{L}1$ adaptive control is applied. The results are plotted in Fig. 5 and 6. In the time interval [0, 52]s, the wearer is passive which can be verified by null EMG measurements for the RF and BF muscles. Notice that there is a small time lag between the current and desired knee joint angles. Starting second 52, the wearer has developed an effort trying to drive the shank-foot-exoskeleton in the same direction as the desired trajectory. This can be verified by the rectus femoris (RF) EMG activity during extension and BF EMG activity during flexion. Note that the control torque has a lower value relative to the passive phase since the exoskeleton is only assisting the wearer. Note also that there is no time lag between the current and desired knee

joint angles. Once the wearer becomes active, the estimated parameters W_1 and W_2 present a sign alteration (cf. Fig. 6).

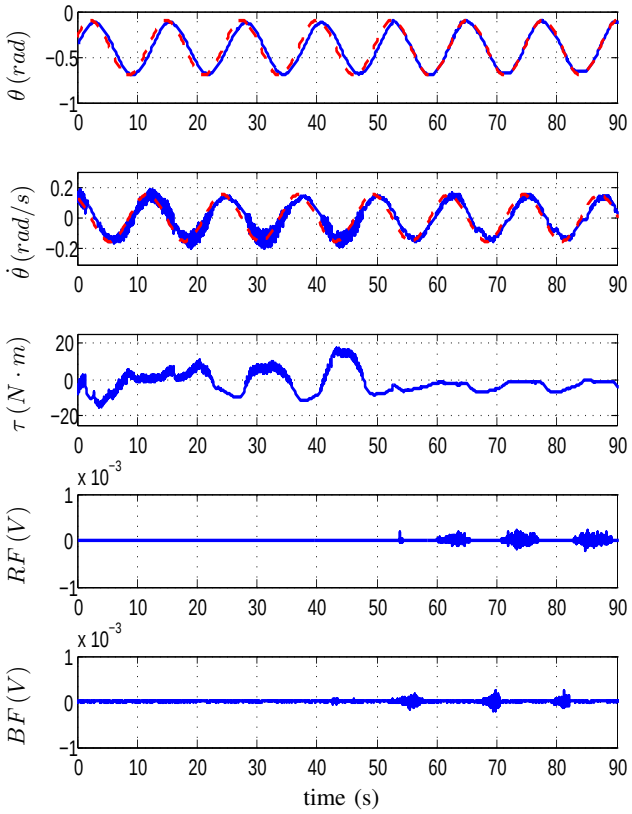

Fig. 5. Classical $\mathcal{L}1$ adaptive control with assistance-as-needed process starting at time 52s: The first plot presents the current (continuous blue line) and desired (dashed red line) knee joint angles, the second plot presents the current (continuous blue line) and desired (dashed red line) knee joint angular velocities, the third plot gives the control torque, the fourth and fifth plots give the RF and BF EMG measurements respectively.

The second experiment consists in applying the augmented $\mathcal{L}1$ adaptive control for the same case study. Results are presented in Fig. 7 and 8. The wearer is passive in the time interval [0,50]s and active, assisted by the exoskeleton thereafter. This can be verified by the EMG measurements in the last two plots of Fig. 7. One can notice that the time lag, observed in the previous experiment with a passive wearer, has vanished thanks to the augmentation of the $\mathcal{L}1$ adaptive controller. The control torque values decrease in the time interval [50,90]s since a part of the effort is delivered by the wearer. Note that the estimated parameters have no sudden variation as W_1 and W_2 of the previous case (cf. Fig. 8).

C. Resistive rehabilitation

The last two experiments can be divided into two phases: the first one presents a passive wearer who is not delivering any active muscular effort and the second phase presents a wearer who is resisting to the exoskeleton's movement towards the desired trajectory.

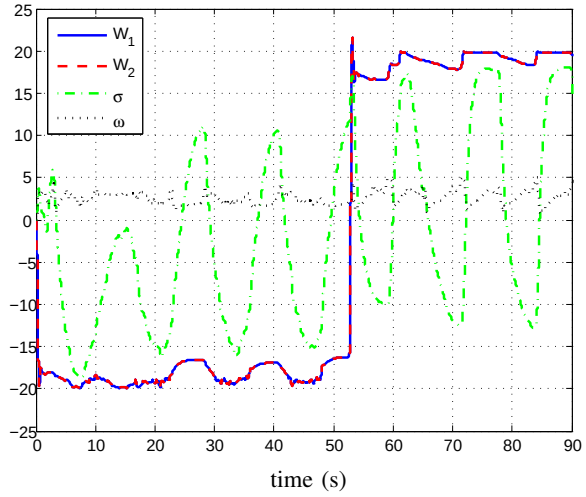

Fig. 6. Classical $\mathcal{L}1$ adaptive control with assistance-as-needed process starting at time 52s: The figure presents the different estimated parameters of the control torque.

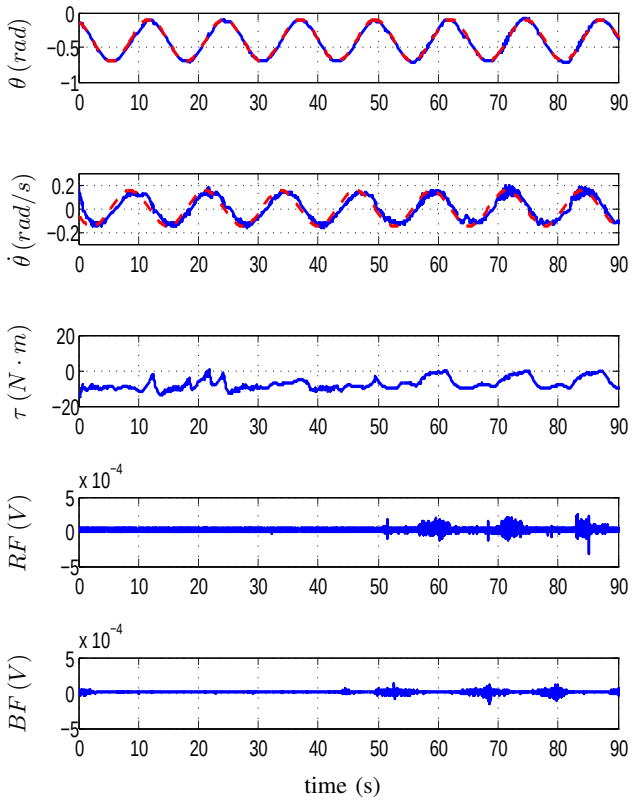

Fig. 7. Augmented $\mathcal{L}1$ adaptive control with assistance-as-needed process starting at time 50s: The first plot presents the current (continuous blue line) and desired (dashed red line) knee joint angles, the second plot presents the current (continuous blue line) and desired (dashed red line) knee joint angular velocities, the third plot gives the control torque, the fourth and fifth plots give the RF and BF EMG measurements respectively.

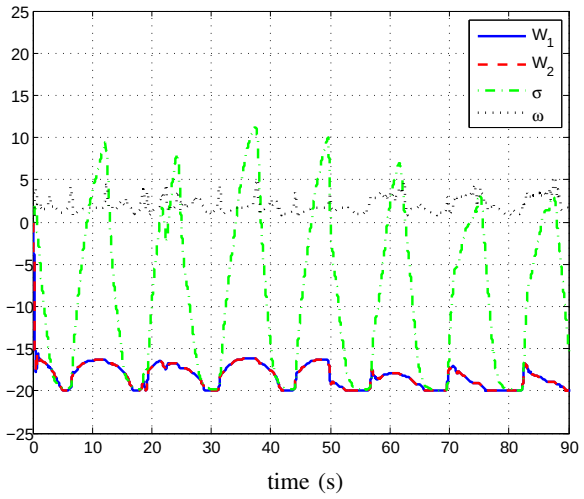

Fig. 8. Augmented $\mathcal{L}1$ adaptive control with assistance-as-needed process starting at time 50s: The figure presents the different estimated parameters of the control torque.

During the third experiment, the classical $\mathcal{L}1$ adaptive control is implemented. The wearer is passive in the time interval [0,55]s and is resisting the exoskeleton's movement towards the desired trajectory after (cf. Fig. 9 and 10). This can be verified by the EMG measurements of the RF and BF muscles. In the time interval [55,90]s, the RF muscle is active during the flexion phase of the exoskeleton and the BF muscle is active during the extension phase. Notice again the time lag between the current and desired knee joint angles since it is the classical $\mathcal{L}1$ adaptive control law that is implemented. Note that the control torque is greater when the wearer is resisting the exoskeleton's movement to overcome this resisting muscular effort and to drive the shank-foot-exoskeleton system towards the desired trajectory. The wearer's resistance has allowed the deviation of the current trajectory from the desired one (first plot of Fig. 9). The resistance of the wearer can also be seen in the estimated parameters plots through the appearance of some oscillations (cf. Fig. 10). i

In the last experiment, the augmented $\mathcal{L}1$ adaptive control is implemented with a passive phase in the time interval [0,49]s followed by a resisting phase in the time interval [49,90]s (cf. Figs. 11 and 12). This can be verified by the EMG measurements of RF and BF muscles. One can notice that the time lag in the knee joint angle tracking has been eliminated. Note that, as in the previous experiment, the control torque has higher values during the resisting phase relative to the passive one. Note also that during the resistive phase, the current knee joint angle does not track accurately the desired one. The estimated parameters (cf. Fig. 12) present less oscillations relative to the classical $\mathcal{L}1$ adaptive control (cf. Fig. 10).

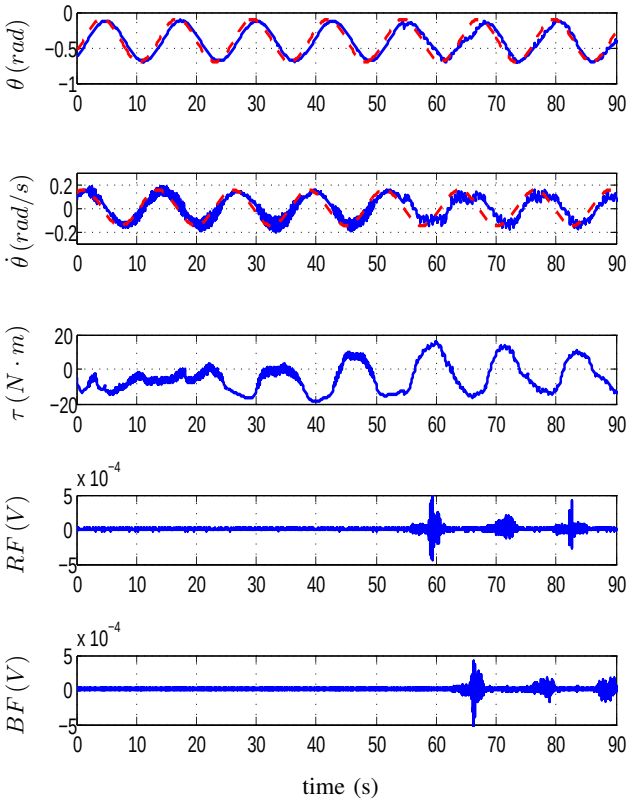

Fig. 9. Classical $\mathcal{L}1$ adaptive control with resistive rehabilitation process strarting at time 55s: The first plot presents the current (continuous blue line) and desired (dashed red line) knee joint angles, the second plot presents the current (continuous blue line) and desired (dashed red line) knee joint angular velocities, the third plot gives the control torque, the fourth and fifth plots give the RF and BF EMG measurements respectively.

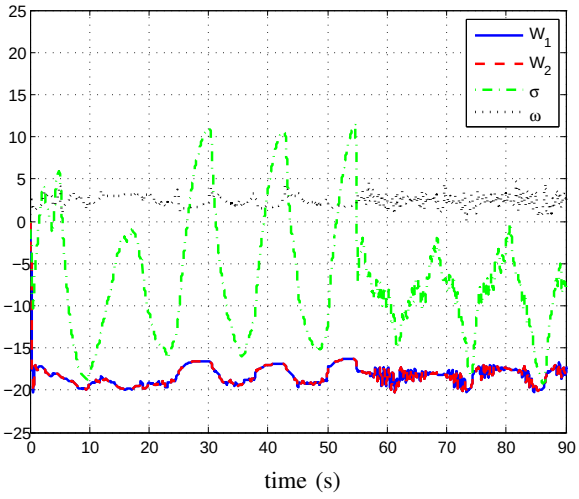

Fig. 10. Classical $\mathcal{L}1$ adaptiive control with resistive rehabilitation process starting at time 55s: The figure presents the different estimated parameters of the control torque.

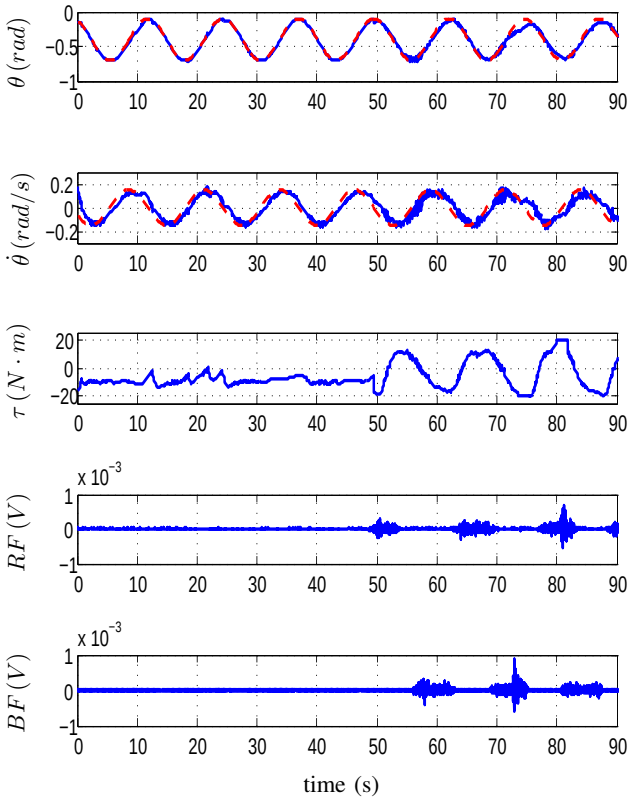

Fig. 11. Augmented $\mathcal{L}1$ adaptive control with resistive rehabilitation process starting at time 49s: The first plot presents the current (continuous blue line) and desired (dashed red line) knee joint angles, the second plot presents the current (continuous blue line) and desired (dashed red line) knee joint angular velocities, the third plot gives the control torque, the fourth and fifth plots give the RF and BF EMG measurements respectively.

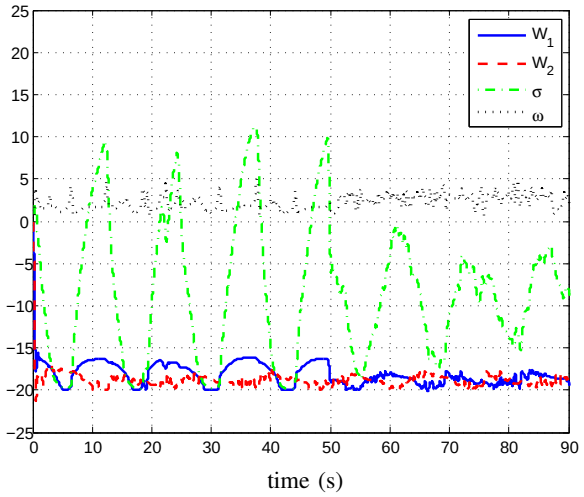

Fig. 12. Augmented $\mathcal{L}1$ adaptive control with resistive rehabilitation process starting at time 49s: The figure presents the different estimated parameters of the control torque.

V. CONCLUSION AND FUTURE WORK

In the present paper, a classical $\mathcal{L}1$ adaptive control is applied to control the lower limb exoskeleton EICOSI. Because of the time lag that this control introduces, an augmented $\mathcal{L}1$ adaptive control by means of a nonlinear proportional controller is proposed. These two control laws are tested in real-time using the exoskeleton EICOSI for assistance-as-needed and resistive rehabilitation case studies while tracking a desired trajectory considered defined by a therapeutic doctor. Experiments have confirmed the presence of a time lag when the classical $\mathcal{L}1$ adaptive control is applied. This time lag has been eliminated when the augmented version of the $\mathcal{L}1$ adaptive control is applied. When performing assistance-as-needed experiments, results have showed that the control torque has a lower value relative to the passive case since the wearer is performing the movement and the exoskeleton is only assisting him. On the other hand, when performing the resistive rehabilitation, the control torque has higher values than the passive case in order to counteract the resistive effort of the wearer and drive the exoskeleton towards the desired trajectory.

Future works consist in applying the $\mathcal{L}1$ adaptive control on the full lower limb exoskeleton for achieving daily living activities like walking, ascending and descending stairs.

REFERENCES

[1] S. Mohammed, Y. Amirat, and H. Rifai, "Lower limb movement assistance through wearable robots: State of the art and challenges," *Advanced Robotics*, vol. 26, no. 1-2, pp. 1–22, 2012.

[2] M. Bortole, A. Venkatakrishnan, F. Zhu, J. Moreno, G. Francisco, J. Pons, and J. Contreras-Vidal, "The H2 robotic exoskeleton for gait rehabilitation after stroke: early findings from a clinical study," *Journal of Neuroengineering and rehabilitation*, vol. 12, no. 54, pp. 1–14, 2015.

[3] H. Kazerooni, J. Racine, L. Huang, and R. Steger, "On the control of the Berkeley lower extremity exeskeleton (BLEEX)," in *Porceedings of the International Conference on Robotics and Automation*, Barcelona, Spain, 2005, pp. 4364–4371.

[4] C. Jansen, J. Windau, P. Bonutti, and M. Brillhart, "Treatment of a knee contracture using a knee orthosis incorporating stress-relaxation techniques," *Journal of Physical Therapy Association*, vol. 76, no. 2, pp. 182–186, 1996.

[5] C. Rudhe, U. Albisser, A. Starkey, M. Curt, and M. Bolliger, "Reliability of movement workspace measurements in a passive arm orthosis used in spinal cord injury rehabilitation," *Journal of Neuroengineering and Rehabilitation*, vol. 9, no. 37, pp. 1–8, 2012.

[6] L. Marchal-Crespo and D. Reinkensmeyer, "Review of control strategies for robotic movement training after neurologic injury," *Journal of Neuroengineering and Rehabilitation*, vol. 6, no. 20, pp. 1–15, 2009.

[7] C. Fleischer and G. Hommel, "A humanexoskeleton interface utilizing electromyography," *IEEE Transations on Robotics*, vol. 24, no. 4, pp. 872–882, 2008.

[8] D. Ferris and C. Lewis, "Robotic lower limb exoskeletons using proportional myoelectric control," in *Proceedings of the IEEE Engineering in Medicine and Biology Society*, Minneapolis, Minnesota, USA, 2009, pp. 2119–2124.

[9] D. Sanz−Merodio, M. Cestari, J. Arevalo, and E. Garcia, "Gait parameter adaptation for lower-limb exoskeletons," in *Proceedings of the InternationalWork-conference on Bioinformatics abd biomedical engineering*, Granada, Spain, 2013, pp. 667–675.

[10] H. Rifai, S. Mohammed, W. Hassani, and Y. Amirat, "Nested saturation based control of an actuated knee joint orthosis," *Mechatronics*, vol. 23, no. 8, pp. 1141–1149, 2013.

[11] K. Shamaei, M. Cenciarini, A. Adams, K. Gregorczyk, J. Schiffman, and A. Dollar, "Design and evaluation of a quasi-passive knee exoskeleton for investigation of motor adaptation in lower extremity joints," *IEEE Transactions on Biomedical Engineering*, vol. 61, no. 6, pp. 1809–1821, 2014.

[12] G. Aguirre-Ollinger, J. Colgate, M. Peshkin, and A. Groswami, "A 1-DOF assistive exoskeleton with virtual negative damping: Effects on the kinematic response of the lower limbs," in *Proceedings of International Conference on Intelligent Robots and Systems*, 2007, pp. 1938–1944.

[13] ——, "Design of an active 1-DOF lower-limb exoskeleton with inertia compensation," *International Journal of Robotics Research*, vol. 30, no. 4, pp. 486–499, 2010.

[14] N. Karavas, A. Ajoudani, N. Tsagarakis, J. Saglia, A. Bicchi, and D. Caldwell, "Tele-impedance based stiffness and motion augmentation for a knee exoskeleton device," in *Proceedings of the IEEE International Conference on Robotics and Automation*, Karlsruhe, Germany, 2013, pp. 2194–2200.

[15] H. Rifai, S. Mohammed, B. Daachi, and Y. Amirat, "Adaptive control of a human-driven knee joint orthosis," in *Proceedings of IEEE Conference on Robotics and Automation (ICRA)*, St. Paul, Minnesota, USA, 2012, pp. 2486–2491.

[16] H. Valley, J. Veneman, E. Van Asseldonk, R. Ekkelenkamp, M. Buss, and H. Van Der Kooij, "Compliant actuation of rehabilitation robots," *IEEE Robotics and Automation Magazine*, vol. 15, no. 3, pp. 60–69, 2008.

[17] N. Hovakimyan and C. Cao, *L1 adapative control theory: Guaranteed robustness with fast adaptation*, R. Smith, Ed. SIAM, 2010.

[18] D. Maalouf, A. Chemori, and V. Creuze, "A new extension of the l1 adaptive controller to drastically reduce the tracking time lags," in *Proceedings of the IFAC Symposium on Nonlinear Control Systems*, Toulouse, France, 2013, pp. 481–486.

[19] ——, "Stability analysis of a new extended l1 controller with experimental validation on an underwater vehicle," in *Proceedings of the IEEE Conference on decision and control*, Florence, Italy, 2013, pp. 6149–6155.

[20] B. Michini and J. How, "L1 adaptive control for indoor autonomous vehicles: design process and flight testing," in *Proceedings of the AIAA Guidance, navigation and control*, Chicago, Illinois, USA, 2009, pp. 1–15.

[21] C. Cao and N. Hovakimyan, "Guaranteed transient performance with l1 adaptive controller for systems with unknown time-varying parameters and bounded disturbances: Part I," in *Proceedings of the American Control Conference*, NewYork, USA, 2007, pp. 3925–3930.

[22] ——, "Stability margins of l1 adaptive controller: Part II," in *Proceedings of the American Control Conference*, NewYork, USA, 2007, pp. 3931–3936.

[23] W. Wang, *PID Controller Design Approaches - Theory, Tuning and Application to Frontier Areas*, M. Vagia, Ed. InTech, 2012.